


## RESEARCH ARTICLE

# Regional white matter hyperintensity volume in Parkinson's disease and associations with the motor signs

Haoting Wu<sup>1</sup>, Hui Hong<sup>1</sup>, Chenqing Wu<sup>1</sup>, Jianmei Qin<sup>1</sup>, Cheng Zhou<sup>1</sup>, Sijia Tan<sup>1</sup>, Xiaojie DuanMu<sup>1</sup>, Xiaojun Guan<sup>1</sup>, Xueqin Bai<sup>1</sup>, Tao Guo<sup>1</sup>, Jingjing Wu<sup>1</sup>, Jingwen Chen<sup>1</sup>, Jiaqi Wen<sup>1</sup>, Zhengye Cao<sup>1</sup>, Ting Gao<sup>2</sup>, Luyan Gu<sup>2</sup>, Peiyu Huang<sup>1</sup>, Xiaojun Xu<sup>1</sup>, Baorong Zhang<sup>2</sup> & Minming Zhang<sup>1</sup> 

<sup>1</sup>Department of Radiology, The Second Affiliated Hospital, Zhejiang University School of Medicine, Hangzhou, 310009, China

<sup>2</sup>Department of Neurology, The Second Affiliated Hospital, Zhejiang University School of Medicine, Hangzhou, 310009, China

## Correspondence

Minming Zhang, Department of Radiology, The Second Affiliated Hospital, Zhejiang University School of Medicine, Hangzhou 310000, China. Tel: +86 571 87315255; Fax: +86 571 88981063; E-mail: [zhangminming@zju.edu.cn](mailto:zhangminming@zju.edu.cn)

Received: 28 November 2022; Revised: 8 June 2023; Accepted: 9 June 2023

*Annals of Clinical and Translational Neurology* 2023; 10(9): 1502–1512

doi: 10.1002/acn3.51839

## Abstract

**Objective:** To determine whether white matter hyperintensity (WMH) volumes in specific regions are associated with Parkinson's disease (PD) compared to non-PD controls, and to assess their impact on motor signs through cross-sectional and longitudinal analyses. **Methods:** A total of 50 PD participants and 47 age- and gender-matched controls were enrolled. All PD participants were followed up for at least 2 years. To detect regions of greater WMH in the PD, the WMH volume of each region was compared with the corresponding region in the control group. Linear regression and linear mixed effects models were respectively used for cross-sectional and longitudinal analyses of the impact of increases in WMH volume on motor signs. **Results:** The PD group had greater WMH volume in the occipital region compared with the control group. Cross-sectional analyses only detected a significant correlation between occipital WMH volume and motor function in PD. Occipital WMH volume positively correlated with the severity of tremor, and gait and posture impairments, in the PD group. During the follow-up period, the participants' motor signs progressed and the WMH volumes remained stable, no longitudinal association was detected between them. The baseline occipital WMH volume cannot predict the progression of signs after adjustment for baseline disease duration and the presence of vascular risk factors. **Interpretation:** PD participants in this study were characterized by greater WMH at the occipital region, and greater occipital WMH volume had cross-sectional associations with worse motor signs, while its longitudinal impact on motor signs progression was limited.

## Introduction

White matter hyperintensities (WMHs) are areas of high signal intensity on T2-weighted fluid-attenuated inversion recovery (T2-FLAIR) magnetic resonance imaging (MRI) images, which are typical signs of small vessel disease.<sup>1</sup> Pathological examination of the tissues corresponding to WMHs may reveal loss of myelin, axons, and oligodendrocytes, microglial activation, lipohyalinosis, arteriosclerosis, vessel wall leakage, and collagen deposition in venular walls.<sup>2–4</sup> Although WMHs are often observed in older adults and were previously thought to be benign changes associated with aging, a contribution to Parkinson's disease (PD) has also been noted.<sup>5,6</sup>

In a recent systematic review, it was mentioned that individuals with PD did not have a higher burden of global WMH compared to controls.<sup>7</sup> However, since most studies rarely include regional detail, it remains unclear whether WMHs are more severe in specific brain regions within PD. The spatial burden of WMHs has been reported to vary between controls and patients with Alzheimer's disease and frontotemporal dementia in previous studies.<sup>8,9</sup> These neurodegenerative diseases share common pathophysiological characteristics with PD, including protein misfolding, prion-like propagation, and progressive accumulation of protein deposition.<sup>10</sup> Those processes underlying neurodegeneration are also involved in WMH-related mechanisms,<sup>11</sup> and have been

demonstrated to produce a different loading pattern of WMHs linked to vascular risk.<sup>12</sup> In this sense, it is possible that PD may have a higher WMH volume than healthy controls in specific brain regions, which needs further investigation.

In addition, evaluated WMH only at global level may be insensitive for signs related to topographically “eloquent”, especially motor signs of PD. Several studies have reported that PD motor signs are related to WMHs located in specific regions, including an association between falls and WMHs located in the temporal region,<sup>13</sup> and associations between frontal WMH burden and axial signs as well as bradykinesia.<sup>14</sup> Furthermore, combining location information in WMH analysis would also improve the understanding of underlying mechanisms of motor signs associated with PD. WMHs are considered to accompany white matter destruction, so detecting a correlation between different motor signs and specific regional WMHs may help identify the structural loop leading to the signs.<sup>15</sup>

The most common approach to evaluate WMH burden in different brain regions was applying visual rating scales.<sup>16,17</sup> Visual rating scales rely heavily on the human eye to detect and describe WMHs in a qualitative or semi-quantitative way. Although some scales categorize WMHs according to their size and quantity with comprehensive standards, they are still limited by rater dependence and can be problematic for detecting longitudinal change, hampered by floor and ceiling effects.<sup>15,18</sup> Recently, automated techniques have been developed to segment and calculate WMH volumes. Algorithm techniques replace the human eye, and 3D reconstruction and computation allow quantitative data on WMHs. These quantification methods are more objective and reliable and can be more sensitive to catch longitudinal changes in WMHs compared with visual WMH ratings.<sup>7,18</sup>

So far, only one study has used automated techniques to analyze regional WMH in Parkinson’s disease, including both cross-sectional and longitudinal data with a sample size of 21 PD participants.<sup>19</sup> However, this study did not find any spatial distribution differences between PD and controls, and did not detect significant cross-sectional or longitudinal associations between regional WMH and motor function. The limited statistical power of this study due to its small sample size and short follow-up time of 18 months may have contributed to these negative findings.

In light of these gaps, we aimed to determine WMH volumes in specific regions associated with PD compared to controls, and to assess their impact on motor signs through cross-sectional and longitudinal analyses. To this end, we enrolled 50 PD participants with a minimum follow-up of 2 years, and used automated techniques to

extract regional WMH volumes in each region of interest, based on a lobar atlas and each subject’s native space.

## Methods

### Participants

In total, 50 PD participants were prospectively enrolled in this study. All participants were diagnosed according to the UK Parkinson’s Disease Society Brain Bank Diagnostic Criteria by a senior neurologist,<sup>20</sup> and none met the diagnostic criteria for vascular parkinsonism.<sup>21</sup> All PD participants had attended clinical follow-up visits for at least 2 years. A group of 47 controls were recruited from the community. Written consent was obtained from all participants after the study was approved by the Medical Ethics Committee of the Second Affiliated Hospital of Zhejiang University School of Medicine.

At baseline, all participants underwent clinical assessments within 5 h of MRI scanning. Motor function was quantified using the Unified Parkinson’s Disease Rating Scale Part III (UPDRS III).<sup>22</sup> According to the UPDRS III score (excluding an action tremor item score  $\leq 3$ ),<sup>23</sup> all controls were under the threshold of possible parkinsonism. For the PD group, tremor (items 20 and 21), rigidity (item 22), bradykinesia (items 23–26), and gait and posture impairment (items 27–30) UPDRS III sub-scores were calculated.<sup>24</sup> Global cognitive function was quantified using the Mini-Mental State Examination (MMSE).<sup>25</sup> On the basis of studies showing that cognitively impaired individuals had higher WMHs,<sup>26</sup> all participants were confirmed to be free of cognitive impairment according to the MMSE, with reference to specific thresholds for the Chinese population (MMSE score  $>17$  for illiterate subjects,  $>20$  for grade school level subjects, and  $>23$  for junior high school and higher education level subjects).<sup>27</sup> All PD participants were evaluated in the “off-state”, that is, after washing out anti-Parkinson medications for at least 12 hours. The total levodopa equivalent daily dose (LEDD) of each PD participant was recorded.<sup>28</sup> The same evaluation instruments were used at all follow-up visits for the PD participants.

We collected information on hypertension, high cholesterol, diabetes, and smoking status from participants based on their self-reported answers. The presence of each vascular risk factor was recorded as a single binary variable. These risk factors are known to contribute to WMHs.<sup>29</sup>

### Image acquisition

All participants underwent MRI scans performed using a 3.0 T scanner (Discovery 750; GE Healthcare, Chicago, IL,

USA) at the baseline visit. The scanner was equipped with an eight-channel brain phased array coil. Scanning modalities included T2-FLAIR and high-resolution 3D sagittal T1-weighted imaging. The T2-FLAIR images were acquired with the following settings: repetition time = 8400 ms; echo time = 152 ms; inversion time = 2100 ms; flip angle = 90°; field of view = 240 mm × 240 mm<sup>2</sup>; matrix = 256 × 256; and slice thickness = 4 mm. T1 images were acquired using a fast spoiled gradient-recalled sequence (echo time = 3.0 ms; repetition time = 7.3 ms; inversion time = 450 ms; flip angle = 11°; field of view = 260 × 260 mm<sup>2</sup>; matrix = 256 × 256; and slice thickness = 1.2 mm). All drug-managed PD participants were scanned during the off-state.

### Calculation of intracranial volume

To scale WMH volumes to head size, the intracranial volume (ICV) was determined by summing the gray matter, white matter, and cerebrospinal fluid volumes for each participant. All volumes were obtained from T1-weighted images using the Computational Anatomy Toolbox in Statistical Parametric Mapping, version 12 (SPM12; <http://www.fil.ion.ucl.ac.uk/spm/software/spm12/>).

### White matter hyperintensity segmentation and calculation

Each participant's WMH was segmented using the lesion prediction algorithm (version 3.0.0; [www.statistical-modelling.de/1st.html](http://www.statistical-modelling.de/1st.html)) in SPM12 and FLAIR images, in accordance with a previous study.<sup>30</sup> We segmented the WMH lesions observed in FLAIR images by estimating the lesion probability for each voxel and then computed native space lesion probability maps (LPMs). The LPMs were then binarized (threshold = 0.5) with a minimal cluster extent of 15 mm<sup>3</sup> under the default settings. To ensure accurate capture of WMHs, all LPMs were visually checked against the FLAIR images and manually corrected by an experienced radiologist on the basis of published standards.<sup>1</sup>

All binarized LPMs were divided into six regions with reference to the Mayo Clinic Adult Lifespan Template (MCALT; <https://www.nitrc.org/projects/mcalt/>), which includes deep gray and white matter, and frontal, temporal, occipital, parietal, and insular regions. The binarized LPM of one participant was firstly computed in the MCALT template space using the respective T1 images, and was then projected back onto individual native space images using the inverse transformation matrices calculated in advanced neuroimaging tools (Fig. 1). Visual checks were performed on all final templates warped to the native space.

On the basis of the LPMs, the WMH volumes in six regions were calculated for each participant. The WMH volume in each region was normalized by dividing it by the corresponding ICV and multiplying by 100,000. The normalized regional WMH volume was log-transformed to ensure normality and then added to a constant of 1 to produce uniformly positive values.<sup>19</sup> The following analyses used the values of WMH volumes after normalization and log transformation.

### Statistical analysis

All of the statistical analyses described below were performed using SPSS (version 26.0; IBM Corp, Armonk, NY, USA) or MATLAB (R2020b; MathWorks, Natick, MA, USA) software. A false discovery rate was applied for multiple comparisons. Two-tailed *p*-values <0.05 were considered statistically significant.

### Group comparison of baseline demographic and clinical data

Cross-sectional comparisons between the PD and the control groups were performed using two-sample *t*-tests for normally distributed continuous variables; otherwise, the Mann–Whitney test was applied. Qualitative variables were compared with chi-squared tests.

### Baseline differences in WMH volumes between the PD and control groups

Generalized linear models were used to compare global and regional WMH volumes between the PD and control groups with adjustment for age, gender, and the presence of each vascular risk factor (including hypertension, high cholesterol, diabetes, and smoking). Regions exhibiting significant group differences in the WMH volume were subjected to the association analyses described below.

### Cross-sectional association between WMH volumes and motor signs at baseline

We first constructed regression models that included global and regional WMH volumes as dependent variables and motor function (UPDRS III total score) as the independent variable. To determine whether disease status influenced the correlations, the group, and the group × WMH interaction were also included as independent variables. Within-group regression analyses were conducted to determine whether there were significant correlations between WMH volumes and motor function in both groups.

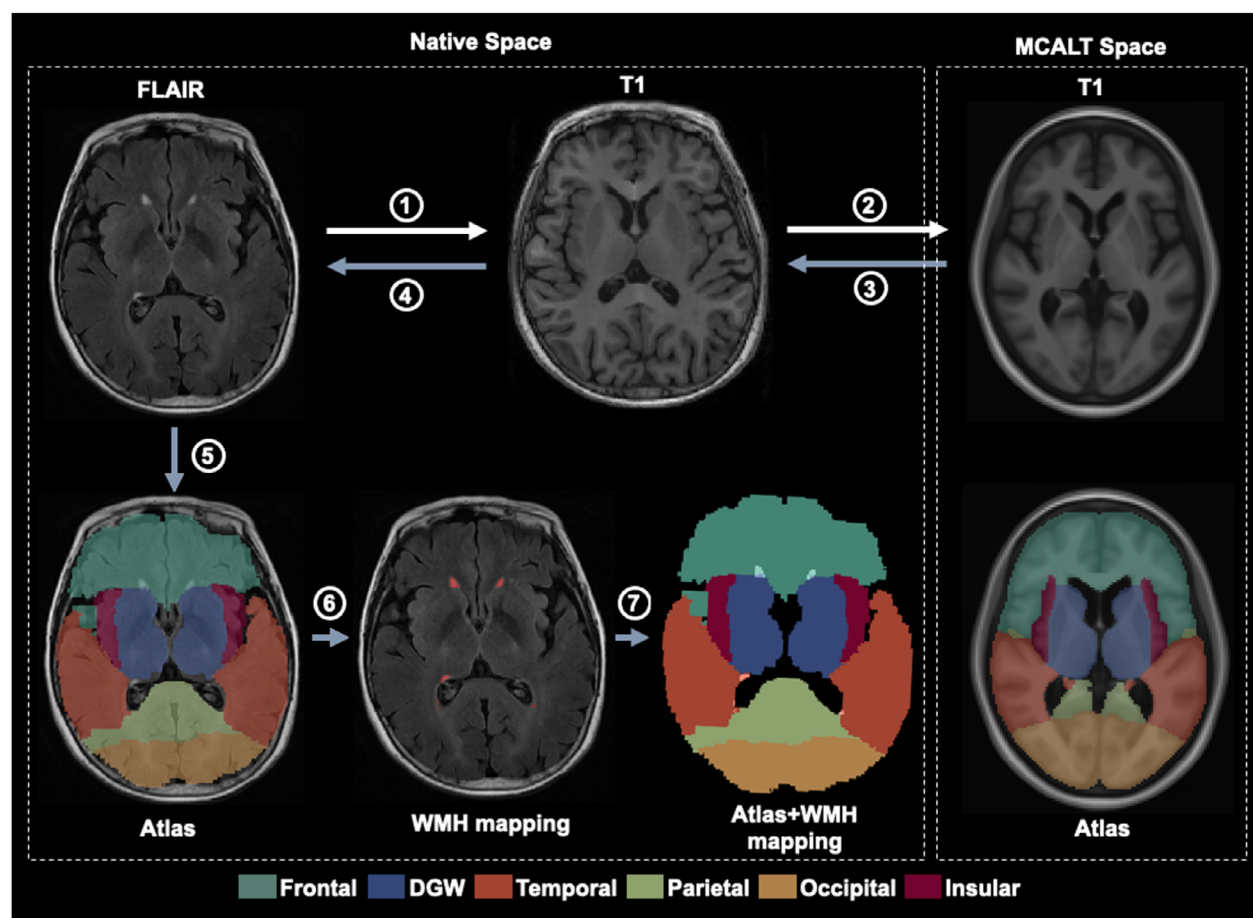


**Figure 1.** Flowchart illustrating how the white matter hyperintensities (WMHs) were divided into six regions on the basis of atlas. Fluid-attenuated inversion recovery (FLAIR) images of each participant were converted into Mayo Clinic Adult Lifespan space by reference to their associated T1 images; transformation matrices were then obtained (steps 1 and 2). Inverse transformation matrices were used to transform the atlas images back into FLAIR images (steps 3–5). Finally, the WMH volume of each region was determined by overlaying the WMH map (segmented from FLAIR images) onto the atlas image in native space (steps 6 and 7). DGW, deep gray and white matter.

The associations of global and regional WMH volumes with four motor signs (UPDRS III sub-scores) were further examined in the PD group. Age, gender, and the presence of each vascular risk factor were included as covariates in all regression analyses. Considering the significant correlation between disease duration and sign severity (Table S1), regression analyses of the PD group included disease duration as an additional covariate. All analyses were rerun with regions not showing group differences in WMH volumes as additional variables.

### Longitudinal association between WMH Volumes and motor signs in PD

In the PD group, we analyzed the changes in WMH volumes and motor signs that occurred during the follow-up period. The following linear mixed effects models were used:

$$\text{Model 1 : WMH}_{ij} \sim \text{Year}_{ij} + \text{Baseline age}_i + \text{Gender}_i + (1 + \text{Year}_{ij} | \text{Participant}_i)$$

$$\text{Model 2 : Sign}_{ij} \sim \text{Year}_{ij} + \text{Baseline age}_i + \text{Gender}_i + (1 + \text{Year}_{ij} | \text{Participant}_i)$$

We also tested for associations between changes in WMH volumes and the progression of motor signs in cases for which WMH volumes and signs showed a significant correlation at baseline:

$$\begin{aligned} \text{Model 3 : Sign}_{ij} \sim & \text{WMH}_{ij} + \text{Baseline age}_i + \text{Gender}_i \\ & + \text{Year}_{ij} + \text{Baseline duration}_i \\ & + \text{Presence of vascular risk factors at baseline}_i \\ & + (1 + \text{Year}_{ij} | \text{Participant}_i) \end{aligned}$$

Finally, we investigated whether baseline WMH volumes were predictive of motor sign progression during

the follow-up period in cases for which WMH volumes and signs showed significant correlations at baseline:

Model 4 :  $\text{Sign}_{ij} \sim \text{Baseline WMH}_i + \text{Baseline age}_i$

+  $\text{Gender}_i + \text{Year}_{ij} + \text{Baseline duration}_i$

+ Presence of vascular risk factors at baseline;

+  $(1 + \text{Year}_{ij} | \text{Participant}_i)$

In these models, subscript  $i$  referred to the  $i$ th participant and  $ij$  referred to participant  $i$  at timepoint  $j$  (in years).  $\text{Year}_{ij}$  was defined as the time interval between the baseline visit and follow-up timepoint  $j$  (in years; baseline = 0). Both the intercept (indicated by 1) and slope of the follow-up year (indicated by “+  $\text{Year}_{ij}$ ”) varied by the participant and were defined as random effects. The baseline age and gender were added to all regression models as additional fixed effects. The baseline duration and the presence of each vascular factor were also included as fixed effects when exploring the longitudinal impact of WMH volumes on signs (Models 3 and 4).

## Results

### Baseline demographic and clinical data

The baseline demographic and clinical data of all participants are summarized in Table 1. PD participants and controls were age- and gender-matched, although the controls had a significantly higher level of education than the PD participants ( $p = 0.037$ ). The PD participants had significantly higher UPDRS III scores than the controls ( $p < 0.001$ ), and the majority of PD participants were at mild to moderate stages (Median = 2.5). The MMSE scores were comparable between two groups ( $p = 0.242$ ), even after adjustment for education level ( $p = 0.332$ ).

### PD participants had greater occipital WMH volume at baseline

The between-group comparison showed that the global WMH volume of the PD and control groups was similar at baseline (1.21 vs. 1.35,  $p = 0.406$ ), but there was a significant difference in the occipital region (2.75 vs. 2.46,  $p = 0.028$ ). And these findings did not change without normalization with ICV. Results are detailed in Figure 2 and Table S2 in the Supplementary Materials. In the within-group comparison, paired  $t$ -tests indicated that the occipital region had greater WMH volume than other five regions ( $p \leq 0.003$ ) in the PD group, but only greater than the WMH volume in deep gray and white matter ( $p < 0.001$ ), temporal region ( $p < 0.001$ ) and insular region ( $p < 0.001$ ) in the control group (Table S3). The WMH frequency maps of two group are shown in Figure S1.

**Table 1.** Baseline demographic and clinical data.

Variables	Controls ( $N = 47$ )	PD ( $N = 50$ )	$p$ value
Age	57.98 (6.84)	58.87 (9.15)	0.586
Education	11 (2–18)	9 (0–18)	0.037*
Gender (M/F)	23/24	29/21	0.419
UPDRS III score	0 (0–3)	17 (4–52)	<0.001*
Hoehn and Yahr Staging	–	2.5 (1–4)	–
Tremor	–	2 (0–11)	–
Rigidity	–	3.5 (0–16)	–
Bradykinesia	–	5 (1–17)	–
Gait and posture impairment	–	2.5 (0–12)	–
MMSE score	29 (23–30)	28 (18–30)	–
Disease duration	–	2.38 (0.22–10.75)	–
LEDD	–	300 (0–1100)	–
Presence of hypertension (yes/no)	10/37	12/38	0.811
Presence of high cholesterol (yes/no)	7/40	3/47	0.191
Presence of diabetes (yes/no)	4/43	8/42	0.359
Presence of smoking (yes/no)	8/39	13/37	0.330
Intracranial volume ( $\text{cm}^3$ )	1467 (140.30)	1534 (144.18)	0.111

Data presented as mean (standard deviation) were compared using a two-sample  $t$ -test (for normally distributed continuous variables), while those presented as median (range) were compared using the Mann–Whitney test. All qualitative variables were compared using the chi-squared test.

LEDD, levodopa equivalent daily dose; MMSE, Mini-Mental State Examination; PD, Parkinson's disease; UPDRS III, Unified Parkinson's Disease Rating Scale Part III.

\* $p < 0.05$ .

### Occipital WMH volume was associated with motor signs in the PD group at baseline

A significant group  $\times$  occipital WMH volume interaction effect on the UPDRS III score was observed ( $\beta = 11.13$ ,  $p = 0.014$ ). The occipital WMH volume was significantly correlated with the UPDRS III scores in the PD group ( $\beta = 11.48$ ,  $p = 0.049$ ), but not in the control group ( $\beta = 0.26$ ,  $p = 0.840$ ).

The association between the occipital WMH volume and UPDRS III score remained significant after adjustment for disease duration ( $\beta = 11.38$ ,  $p = 0.008$ ). Further analysis demonstrated that occipital WMH volume correlated with tremor severity ( $\beta = 2.53$ ,  $p = 0.018$ , Fig. 3A) and gait and posture impairment severity ( $\beta = 2.01$ ,  $p = 0.018$ , Fig. 3D).

There was no group  $\times$  global WMH volume or group  $\times$  other regional WMH volumes interaction effect on the



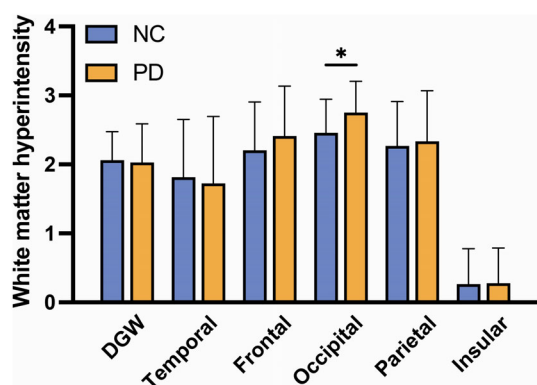


**Figure 2.** Comparison of baseline white matter hyperintensity (WMH) volumes between Parkinson's disease (PD) participants and controls. All WMH volumes were normalized by the intracranial volume and log-transformed. The bar shows mean and standard deviation values for the PD (blue) and controls (yellow) across six regions. PD participants had greater WMH volumes in the occipital region compared with controls (marked with "\*"). No significant differences were detected between the two groups in other regions. DGW, deep gray and white matter.

UPDRS III score (Table S4). Global WMH volume and WMH volumes in other regions were not associated with the UPDRS III score in either group (Table S4). No

motor sign was correlated with the global WMH volume or other regional WMH volumes (Table S5).

### Longitudinal changes of regional WMH volume and motor signs in the PD group

The median follow-up time for the PD group was 3.31 years (range: 2.03–7.35 years) and the median number of follow-up visits was 3 (range: 2–5). The longitudinal changes of motor function and global WMH volume are shown in Figure 4. During the follow-up period, the motor function of PD participants worsened ( $\beta$  of follow-up year: 1.279,  $p = 0.005$ ) and all motor signs progressed ( $\beta$  of follow-up year: 0.145–0.412,  $p \leq 0.046$ ), but none of the regional and global WMH volumes changed ( $\beta$  of follow-up year: 0.0007–0.022,  $p = 0.640$ ) (Detailed in Table 2 and Figure 4).

There was no correlation between the change in occipital WMH volume and tremor progression ( $\beta = -0.68$ ,  $p = 0.525$ ), or between the change in occipital WMH volume and progression of gait and posture impairment ( $\beta = 0.81$ ,  $p = 0.525$ ). These results did not change without adjustment for disease duration, the presence of vascular risk factors, or both (Table S6).

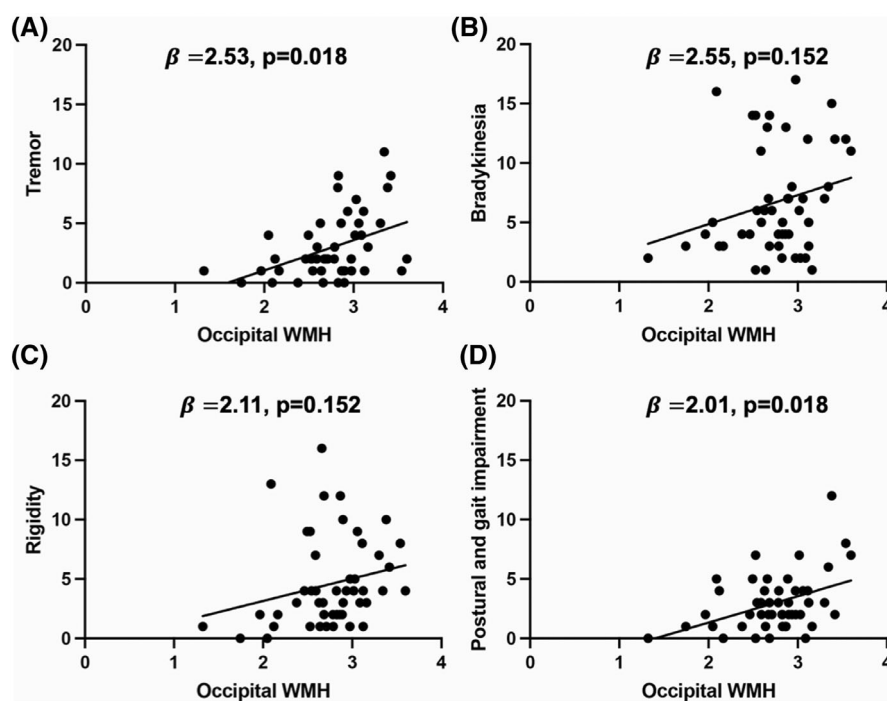


**Figure 3.** Association between motor signs and occipital white matter hyperintensity (WMH) volume in Parkinson's disease participants at baseline. All WMH volumes were normalized by the intracranial volume and log-transformed. The occipital WMH volume was significantly correlated with tremor (A) and gait/posture impairment (D) after adjustment for age, gender, vascular risk factors and disease duration, but not with bradykinesia (B) or rigidity (C). All  $p$ -values were corrected by the false discovery rate.

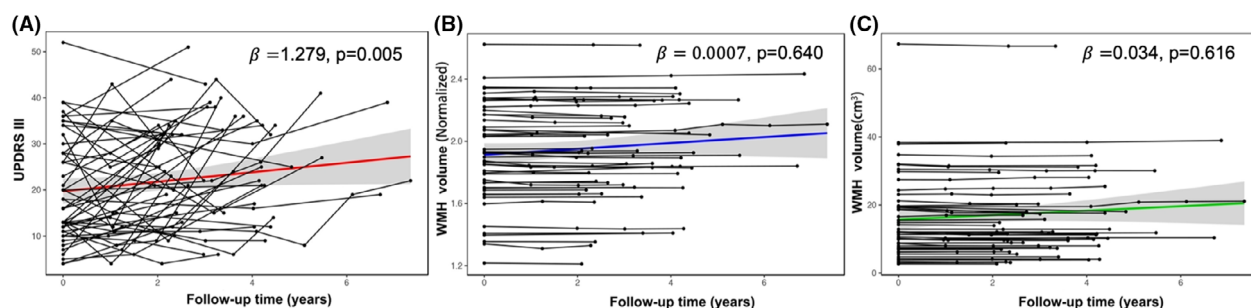


**Figure 4.** Longitudinal changes in motor function and global white matter hyperintensity (WMH) volume. The red, blue, and green lines represent the changes in motor function (A), global WMH volume (B), and absolute global WMH volume (before normalization and log transformation, C), respectively, in the Parkinson's disease group. The black dots and connected lines indicate the changes of variables during follow-up at the subject level. Motor function was evaluated using the Unified Parkinson's Disease Rating Scale Part III (UPDRS III).

**Table 2.** Longitudinal evaluation of regional WMH volumes and motor signs in Parkinson's disease.

Variables	$\beta$ of follow-up year	<i>p</i> value
WMH volumes		
Global	0.0007	0.640
Deep gray and white matter	0.016	0.640
Temporal	0.022	0.640
Frontal	0.009	0.640
Occipital	0.005	0.640
Parietal	0.010	0.640
Insular	0.020	0.640
Motor variables		
UPDRS III score	1.279	0.005*
Tremor	0.292	0.018*
Bradykinesia	0.404	0.018*
Rigidity	0.412	0.013*
Postural and gait impairment	0.145	0.046*

All white matter hyperintensity (WMH) volumes were normalized by intracranial volume and log-transformed. All *p*-values were corrected by the false discovery rate.

UPDRS III, Unified Parkinson's Disease Rating Scale Part III.

\**p* < 0.05.

### Prediction of PD progression on the basis of the baseline occipital WMH volume

The baseline occipital WMH volume cannot predict the progression of tremor ( $\beta = -0.80$ ,  $p = 0.288$ ) or gait and posture impairment ( $\beta = -0.05$ ,  $p = 0.898$ ) after adjustment for baseline disease duration and the presence of vascular risk factors. Additional analyses showed that the prediction of signs progression on the basis of the baseline occipital WMH was only independent of baseline age and gender (Table 3).

## Discussion

The PD participants in this study showed greater WMH volume in the occipital region compared with the controls. The cross-sectional correlation between WMH volume and motor function was detected only at the occipital region in PD and further analyses demonstrated that occipital WMH volume was positively correlated with the severity of tremor and gait and posture impairment. The cross-sectional impact of occipital WMH on these signs was independent of disease duration and presence of vascular risk factors. During the follow-up period, the participants' motor signs progressed and the WMH volumes remained stable, no longitudinal association was detected between them. And the baseline occipital WMH volume cannot predict the worsening of tremor or gait and posture impairment during follow-up after adjustment for baseline disease duration and the presence of vascular risk factors. Our results demonstrated the region specific of association of WMHs with PD, and thus suggest that the location of WMHs should be noted in future studies.

The results suggested that the pattern of WMH burden was different between the PD and control groups, with occipital WMH volume being higher in the PD group compared to both non-PD controls and other regions in the PD group. This finding indicated that the WMH burden in the PD group was characterized by greater involvement of the occipital region. The exact cause of this phenomenon is unknown, but it may be related to decreased cerebral blood flow and accumulation of amyloid- $\beta$ . Previous research suggests that increased WMH burden is related to decreased cerebral blood flow,<sup>31</sup> and PD reportedly showed decreased occipital cortical perfusion.<sup>31,32</sup> Additionally, the WMH that occurred in the occipital region was specific to the progressive accumulation of amyloid- $\beta$  process,<sup>12</sup> and PD had been

**Table 3.** Prediction of sign progression on the basis of baseline variables including the occipital WMH volume.

Variables	Tremor			Gait and posture impairment					
	$\beta$	$\rho$	$\beta$	$\rho$	$\beta$	$\rho$	$\beta$	$\rho$	$\beta$
Occipital WMH	-0.80	0.288	1.56	0.026*	-0.53	0.824	-0.49	0.512	-0.05
Age	-0.03	0.901	0.01	0.785	-0.01	0.956	0.002	0.959	-0.004
Gender	1.72	0.120	-0.30	0.682	1.26	0.088	0.79	0.208	-0.31
Year	0.20	0.539	0.28	0.036*	-0.09	0.566	-0.10	0.629	0.22
Baseline duration	0.18	0.536	-	-	0.20	0.108	-	-	0.02
Smoking	-0.07	0.940	-	-	-	-	0.02	0.980	-0.30
Hypertension	0.13	0.893	-	-	-	-	0.88	0.352	-0.09
Diabetes	0.13	0.912	-	-	-	-	-0.70	0.415	1.61
High cholesterol	0.68	0.794	-	-	-	-	0.83	0.522	0.31

Occipital white matter hyperintensity (WMH) volume was normalized by intracranial volume and log-transformed. All  $p$ -values were corrected by the false discovery rate. "-": means this variable is not included in the regression.

\*  $p < 0.05$ .

shown to have a lower cerebrospinal fluid amyloid- $\beta$  burden than controls even in the early disease stage.<sup>33</sup>

The WMH volume of PD and controls did not differ at the global level, which was consistent with the result of the recent meta-analysis.<sup>7</sup> However, it was important to note that the global WMH volume observed in our study was comparatively lower than that reported in the meta-analysis, which could be attributed to the younger age of our participants. Additionally, contrary to a separate study that reported a higher WMH burden in the anterior deep white matter,<sup>34</sup> we did not detect significant differences between our PD and control groups in other regions. It should be noted that the study employed a coordinate-based approach rather than a standardized lobar atlas to delineate the WMH regions, and this methodological difference may account for the observed discrepancies in regional characterization.

A significant correlation between the UPDRS III score and occipital WMH volume was detected within PD at baseline. An effect of higher occipital WMH volume to severe UPDRS III score only determined at PD, but not in NC. A significant interaction between group and occipital WMH revealed a relationship between occipital WMH volume and global motor impairment in PD. We further investigated the impact of occipital WMH volume on motor signs in PD. Results of cross-sectional analyses demonstrated that occipital WMH volume was associated with greater impairment of gait and posture and tremor at baseline. Previous research had suggested that WMH volume was related to microstructural changes in white matter,<sup>35</sup> therefore WMH located in the occipital region have potential to affect communication between the occipital region and other regions. The occipital region contained the center of the visual information processing system.<sup>36</sup> Its contribution to adjusting gait by mapping the spatial relationship of objects and providing visual guidance to the motor control system had been confirmed.<sup>37</sup> Recent research using other imaging modalities has also detected a correlation between the occipital region and tremor in PD.<sup>38–40</sup> These findings provide further support for the notion that the visual area is relevant to motor impairment in PD.

A previous study had detected the impact of frontal WMH on bradykinesia and axial impairment using visual rating scales,<sup>14</sup> but no such correlation was found in our study, which used a different approach for WMH burden evaluation and region identification. Additionally, differences in the enrolled subjects between the two studies may have contributed to the discrepant findings. It is worth noting that the previous study only included de novo PD participants who had never received dopamine medication, while our study included treated participants.



Although our treated participants had been evaluated during off-state, the long duration impact of levodopa can still improve the motor signs,<sup>41</sup> which may further impact the correlation between regional WMH and motor signs.

Although we enrolled more PD subjects with longer follow-up compared to the study mentioned in the introduction,<sup>19</sup> we still did not detect a significant longitudinal correlation between the progression of motor signs and occipital WMH volume. The median follow-up time of PD subjects enrolled in our study was 3.31 years, which have not been long enough to measure the change of regional WMH volume. Additional analyses showed that the baseline occipital WMH volume failed to predict the progression of motor signs after adjusting for baseline disease duration and the presence of vascular risk factors. Previous studies have demonstrated a correlation between motor signs progression and disease duration, as well as the presence of vascular risk factors. Longer disease duration has been shown to drive faster progression of motor impairment in PD, even during short follow-up periods.<sup>42</sup> The presence of vascular risk factors has also been noted to correlate with worse motor signs.<sup>43</sup> These results suggest that the impact of occipital WMH on motor signs progression may be limited and can be affected by baseline characteristics.

Our study had several limitations that need to be addressed. First, the FLAIR images used in this study were relatively thick, which may have affected the accuracy of WMH quantification due to the irregular pattern of WMH across slices. Second, we suggested that the vascular risk factors of the participants should be better characterized, including blood pressure readings, pack-years of smoking, and total cholesterol, as this could aid in exploring their impact on the correlation between regional WMH and motor signs. Third, since the accumulation rate of WMH is relatively slow,<sup>44</sup> this short follow-up times of PD participants may not have allowed for measurable increases in WMH, the longitudinal associations between regional WMHs and motor signs could have been analyzed more effectively with a longer follow-up. Finally, these findings also need to be validated in advanced PD to determine the role of regional WMH in the advanced stage.

In summary, our findings suggested that PD participants had greater WMH volume in the occipital region, which was associated with worsened motor signs in a cross-sectional manner. However, the longitudinal impact of occipital WMH on motor sign progression may be limited. Future studies with larger sample sizes and longer follow-up periods are needed to better understand the relationship between regional WMH and motor sign progression in PD.

## Acknowledgements

This work was supported by the National Natural Science Foundation of China (Grant Nos. 82271935, 81971577, 82171888, 82202091, and 82001767), Natural Science Foundation of Zhejiang Province (Grant No. LY22H180002 and LQ21H180008), and 13th Five-year Plan for National Key Research and Development Program of China (Grant No. 2016YFC1306600). We thank Michael Irvine, Ph.D., from Liwen Bianji (Edanz) ([www.liwenbianji.cn](http://www.liwenbianji.cn)) and Adrian Neal for editing the English text of a draft of this manuscript.

## Conflict of Interest

The authors have no conflicts of interest to declare.

## Author Contributions

H.T.W. contributed to the study design, imaging processing, statistical analyses, and original manuscript. H.T.W., H.H., C.Q.W., J.M.Q., C.Z., S.J.T., X.J.D.M., X.J.G., X.Q.B., T.G., J.J.W., J.W.C., J.Q.W., Z.Y.C., T.G., L.Y.G., and B.R.Z. contributed to the acquisition and analysis of data. H.H., C.Q.W., C.Z., and X.J.G. contributed to manuscript drafting. P.Y.H., X.J.X., and M.M.Z. contributed to supervision and manuscript revision. Interpretation of the results and final version approval: all authors.

## References

1. Wardlaw JM, Smith EE, Biessels GJ, et al. Neuroimaging standards for research into small vessel disease and its contribution to ageing and neurodegeneration. *Lancet Neurol.* 2013;12:822-838.
2. Gouw AA, Seewann A, Vrenken H, et al. Heterogeneity of white matter hyperintensities in Alzheimer's disease: post-mortem quantitative MRI and neuropathology. *Brain.* 2008;131:3286-3298.
3. Roseborough AD, Langdon KD, Hammond R, et al. Post-mortem 7 Tesla MRI detection of white matter hyperintensities: a multidisciplinary voxel-wise comparison of imaging and histological correlates. *Neuroimage Clin.* 2020;27:102340.
4. Humphreys CA, Smith C, Wardlaw JM. Correlations in post-mortem imaging-histopathology studies of sporadic human cerebral small vessel disease: a systematic review. *Neuropathol Appl Neurobiol.* 2021;47:910-930.
5. Veselý B, Rektor I. The contribution of white matter lesions (WML) to Parkinson's disease cognitive impairment symptoms: a critical review of the literature. *Parkinsonism Relat Disord.* 2016;22(Suppl 1):S166-S170.
6. Veselý B, Antonini A, Rektor I. The contribution of white matter lesions to Parkinson's disease motor and gait

- symptoms: a critical review of the literature. *J Neural Transm (Vienna)*. 2016;123:241-250.
7. Butt A, Kamtchum-Tatuene J, Khan K, et al. White matter hyperintensities in patients with Parkinson's disease: a systematic review and meta-analysis. *J Neurol Sci*. 2021;426:117481.
  8. Desmarais P, Gao AF, Lanctôt K, et al. White matter hyperintensities in autopsy-confirmed frontotemporal lobar degeneration and Alzheimer's disease. *Alzheimers Res Ther*. 2021;13:129.
  9. Brickman AM, Provenzano FA, Muraskin J, et al. Regional white matter hyperintensity volume, not hippocampal atrophy, predicts incident Alzheimer disease in the community. *Arch Neurol*. 2012;69:1621-1627.
  10. Soto C, Pritzkow S. Protein misfolding, aggregation, and conformational strains in neurodegenerative diseases. *Nat Neurosci*. 2018;21:1332-1340.
  11. Paolini Paoletti F, Simoni S, Parnetti L, Gaetani L. The contribution of small vessel disease to neurodegeneration: focus on Alzheimer's disease, Parkinson's disease and multiple sclerosis. *Int J Mol Sci*. 2021;22:4958.
  12. Pålhaugen L, Sudre CH, Tecelao S, et al. Brain amyloid and vascular risk are related to distinct white matter hyperintensity patterns. *J Cereb Blood Flow Metab*. 2021;41:1162-1174.
  13. Ciliz M, Sartor J, Lindig T, et al. Brain-area specific white matter hyperintensities: associations to falls in Parkinson's disease. *J Parkinsons Dis*. 2018;8:455-462.
  14. Jeong SH, Lee HS, Jung JH, et al. White matter hyperintensities, dopamine loss, and motor deficits in De novo Parkinson's disease. *Mov Disord*. 2021;36:1411-1419.
  15. Bohnen NI, Albin RL. White matter lesions in Parkinson disease. *Nat Rev Neurol*. 2011;7:229-236.
  16. Scheltens P, Barkhof F, Leys D, et al. A semiquantitative rating scale for the assessment of signal hyperintensities on magnetic resonance imaging. *J Neurol Sci*. 1993;114:7-12.
  17. Wahlund LO, Barkhof F, Fazekas F, et al. A new rating scale for age-related white matter changes applicable to MRI and CT. *Stroke*. 2001;32:1318-1322.
  18. van den Heuvel DM, ten Dam V, de Craen AJ, et al. Measuring longitudinal white matter changes: comparison of a visual rating scale with a volumetric measurement. *AJNR Am J Neuroradiol*. 2006;27:875-878.
  19. Pozorski V, Oh JM, Okonkwo O, et al. Cross-sectional and longitudinal associations between total and regional white matter hyperintensity volume and cognitive and motor function in Parkinson's disease. *Neuroimage Clin*. 2019;23:101870.
  20. Hughes AJ, Daniel SE, Kilford L, Lees AJ. Accuracy of clinical diagnosis of idiopathic Parkinson's disease: a clinico-pathological study of 100 cases. *J Neurol Neurosurg Psychiatry*. 1992;55:181-184.
  21. Zijlmans JC, Daniel SE, Hughes AJ, Révész T, Lees AJ. Clinicopathological investigation of vascular parkinsonism, including clinical criteria for diagnosis. *Mov Disord*. 2004;19:630-640.
  22. status and recommendations. The unified Parkinson's disease rating scale (UPDRS). *Mov Disord*. 2003;18:738-750.
  23. Berg D, Postuma RB, Adler CH, et al. MDS research criteria for prodromal Parkinson's disease. *Mov Disord*. 2015;30:1600-1611.
  24. Lee Y, Ko J, Choi YE, et al. Areas of white matter hyperintensities and motor symptoms of Parkinson disease. *Neurology*. 2020;95:e291-e298.
  25. Folstein MF, Folstein SE, McHugh PR. "Mini-mental state". A practical method for grading the cognitive state of patients for the clinician. *J Psychiatr Res*. 1975;12:189-198.
  26. Hu HY, Ou YN, Shen XN, et al. White matter hyperintensities and risks of cognitive impairment and dementia: a systematic review and meta-analysis of 36 prospective studies. *Neurosci Biobehav Rev*. 2021;120:16-27.
  27. Li H, Jia J, Yang Z. Mini-mental state examination in elderly Chinese: a population-based normative study. *J Alzheimers Dis*. 2016;53:487-496.
  28. Tomlinson CL, Stowe R, Patel S, Rick C, Gray R, Clarke CE. Systematic review of levodopa dose equivalency reporting in Parkinson's disease. *Mov Disord*. 2010;25:2649-2653.
  29. Wardlaw JM, Allerhand M, Doubal FN, et al. Vascular risk factors, large-artery atheroma, and brain white matter hyperintensities. *Neurology*. 2014;82:1331-1338.
  30. Gaubert M, Lange C, Garnier-Crussard A, et al. Topographic patterns of white matter hyperintensities are associated with multimodal neuroimaging biomarkers of Alzheimer's disease. *Alzheimers Res Ther*. 2021;13:29.
  31. Melzer TR, Watts R, MacAskill MR, et al. Arterial spin labelling reveals an abnormal cerebral perfusion pattern in Parkinson's disease. *Brain*. 2011;134:845-855.
  32. Syrimi ZJ, Vojtisek L, Eliasova I, et al. Arterial spin labelling detects posterior cortical hypoperfusion in non-demented patients with Parkinson's disease. *J Neural Transm (Vienna)*. 2017;124:551-557.
  33. Stav AL, Aarsland D, Johansen KK, Hessen E, Auning E, Fladby T. Amyloid- $\beta$  and  $\alpha$ -synuclein cerebrospinal fluid biomarkers and cognition in early Parkinson's disease. *Parkinsonism Relat Disord*. 2015;21:758-764.
  34. de Schipper LJ, Hafkemeijer A, Bouts MJRJ, et al. Age- and disease-related cerebral white matter changes in patients with Parkinson's disease. *Neurobiol Aging*. 2019;80:203-209.
  35. Zeng W, Chen Y, Zhu Z, et al. Severity of white matter hyperintensities: lesion patterns, cognition, and microstructural changes. *J Cereb Blood Flow Metab*. 2020;40:2454-2463.
  36. Guan X, Zeng Q, Guo T, et al. Disrupted functional connectivity of basal ganglia across tremor-dominant and

- akinetic/rigid-dominant Parkinson's disease. *Front Aging Neurosci.* 2017;9:360.
37. Kravitz DJ, Saleem KS, Baker CI, Mishkin M. A new neural framework for visuospatial processing. *Nat Rev Neurosci.* 2011;12:217-230.
  38. Benito-León J, Serrano JJ, Louis ED, et al. Tremor severity in Parkinson's disease and cortical changes of areas controlling movement sequencing: a preliminary study. *J Neurosci Res.* 2018;96:1341-1352.
  39. Zhang D, Liu X, Chen J, Liu B, Wang J. Widespread increase of functional connectivity in Parkinson's disease with tremor: a resting-state fMRI study. *Front Aging Neurosci.* 2015;7:6.
  40. Xiong Y, Han D, He J, et al. Correlation of visual area with tremor improvement after MRgFUS thalamotomy in Parkinson's disease. *J Neurosurg.* 2022;136:681-688.
  41. Cilia R, Cereda E, Akpalu A, et al. Natural history of motor symptoms in Parkinson's disease and the long-duration response to levodopa. *Brain.* 2020;143:2490-2501.
  42. Chahine LM, Siderowf A, Barnes J, et al. Predicting progression in Parkinson's disease using baseline and 1-year change measures. *J Parkinsons Dis.* 2019;9:665-679.
  43. Malek N, Lawton MA, Swallow DMA, et al. Vascular disease and vascular risk factors in relation to motor features and cognition in early Parkinson's disease. *Mov Disord.* 2016;31:1518-1526.
  44. Cai M, Jacob MA, van Loenen MR, et al. Determinants and temporal dynamics of cerebral small vessel disease: 14-year follow-up. *Stroke.* 2022;53:2789-2798.

## Supporting Information

Additional supporting information may be found online in the Supporting Information section at the end of the article.

### Appendix S1.